Analysis of visual modulation sensitivity. IV. Validity of the Ferry–Porter law

Christopher W. Tyler and Russell D. Hamer

Smith-Kettlewell Eye Research Institute, 2232 Webster Street, San Francisco, California 94115

Received October 20, 1986; accepted September 18, 1989

The maximum flicker frequency was determined over a 5+6-log-unit range of retinal illuminance for a stimulus configuration designed to isolate the linear response from long-wavelength (R) cones. For a particular retinal location, the data conformed to the Ferry–Porter law and departed significantly from the predictions of the diffusion equation. The slope of the function was an invariant characteristic and was unaffected by stimulus intensity or area, modulation waveform, or modulation amplitude. However, the slope varied substantially with retinal locus, increasing by more than a factor of 2 between the foveola and 35° eccentricity. This increase shows that the time constant of the linear, unadapted visual response decreases with increasing eccentricity. The difference between foveola and periphery remained at high spatial frequencies, implying that it was not attributable to lateral inhibitory effects.

1. INTRODUCTION

The relationship between the maximum frequency of flicker detection and stimulus intensity defines the limiting temporal response of the visual system. It is therefore of both theoretical and practical interest to determine this relationship as precisely as possible. One formulation is the Ferry–Porter law, under which the maximum, or critical, flicker frequency (CFF) increases as the logarithm of the luminous intensity, L:

$$\mathrm{CFF} = k(\log L - \log L_0), \tag{1}$$

where $L > L_0$ and with k having a typical value of ~12 Hz/decade. L_0 is the threshold intensity.

Even at its inception the Ferry–Porter law was measured over a limited range, and it has since been regarded as only an approximation to the variation of CFF over the full range of intensities. Ferry,[1] following the observations of Plateau,[2] originally measured flicker frequency over a range of 1.4 log units of intensity (varied by setting a candle at different distances from the viewed surface). Porter,[3] while replicating the high-intensity portion of the function, found a slower rate of decrease below 0.6 log cd/m^2. Porter's result was substantiated by Ives[4] and subsequent investigators for conditions involving some degree of peripheral stimulation.[5–7] It can be explained in terms of a high-intensity portion mediated by cones and a low-intensity portion representing the intrusion of rods with a greater sensitivity but with limited flicker resolution. Figure 1A summarizes the results of these early psychophysical studies.

The presence of rod intrusion in such results raises the question of how far the Perry–Porter law would apply to stimulation of a single isolated receptor system, without interference from other receptor types. This question was addressed to some extent in Ferry's original study, in that he used monochromatic test lights with wavelengths from 430 to 690 nm. However, the 1.4-log-unit range of intensities that he used apparently did not extend to the scotopic region. Hecht and Schlaer[5] performed a similar study with monochromatic lights in a centrally viewed, 19° test field, from 450 to 660 nm. They found the rod and cone portions of the curve to shift in accordance with the different spectral sensitivities of the two systems, but even for long wavelengths (670 nm) the rod-mediated portion did not completely disappear. With a large test field at this wavelength, rod sensitivity may still be slightly greater than cone sensitivity at low frequencies, so the rods may have still influenced the flicker results.

We therefore designed stimulus conditions that could completely eliminate rod mediation of the response, to permit determination of the validity of the Ferry–Porter law over a wide range of intensities for a single receptor type. Monochromatic light with a wavelength of 660 nm was used to maximize stimulation of the long-wavelength-sensitive R cones. Two conditions were chosen. The first was a 0.5° field in the central fovea, which is anatomically the only totally rod-free region in the retina.[13,14] The second was a 5.7° field at 35° in the temporal field. To prevent rod intrusion in this condition, and G-cone intrusion in the foveal condition, we used a hemispheric white surround that was photopically equiluminant with the stimulus. This also had the effect of minimizing detection by stray light spreading from the stimulus to other retinal locations.

A. Theoretical Considerations

The theoretical interest of this determination lies in its relevance to the receptor dynamics underlying the flicker results. Kelly[15] followed Veringa[16] in suggesting that the Ferry–Porter law is merely an approximation to the principle that

$$\mathrm{CFF}^p = k'(\log L - \log L_0), \tag{2}$$

where $p = 0.5$ and $L > L_0$.

This is the square-root law of CFF versus intensity, which was originally proposed by Charpentier.[17] Kelly[15] showed that this relation can be derived as a simple solution to the diffusion equation for receptor dynamics,[4,18] based on the concept of spatiotemporal diffusion of a postulated photo-

0740-3232/90/040743-16$02.00

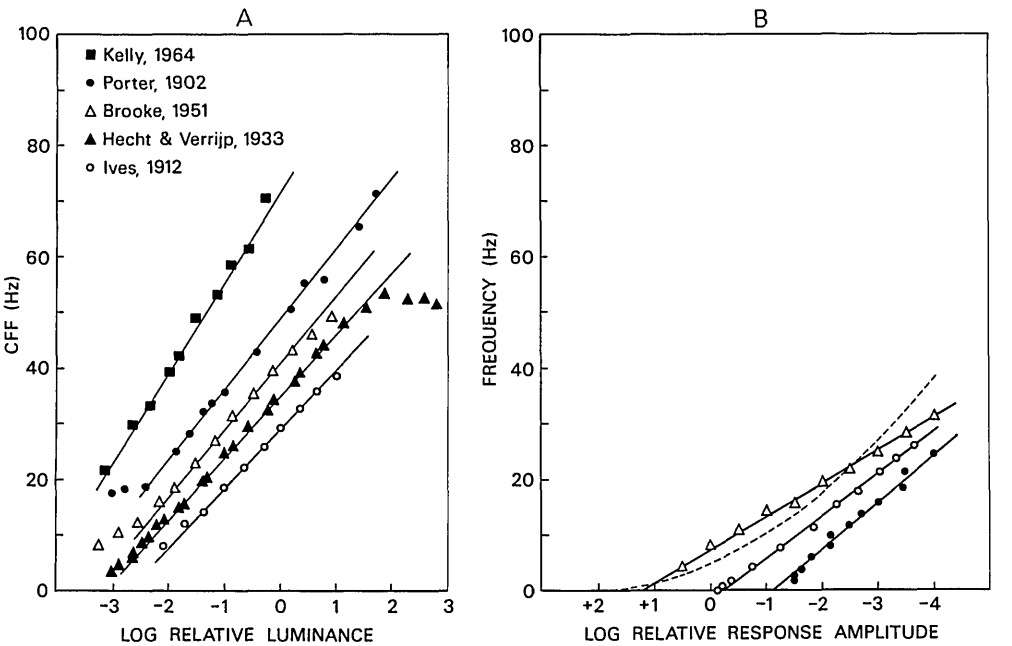

Fig. 1. A, CFF versus intensity data from previous psychophysical studies. Filled circles, Porter[3]; open circles, Ives[4]; filled triangles, Hecht and Verrijp[8]; open triangles, Brooke[9]; filled squares, Kelly[7]. Data sets are placed arbitrarily on the relative luminance abscissa. Straight lines, Ferry–Porter functions fitted by inspection. B, CFF versus intensity data from previous physiological studies. Filled circles, CFF measurements from limulus ommatidia[10]; open circles, CFF measurements from turtle horizontal cell responses[11]; open triangles, CFF estimates from Fourier transforms of turtle cone responses[12]; together with the best-fitting square-root function (dashed curve). Straight line, best-fitting Ferry–Porter functions.

product within the outer segment of the receptor. It turns out that it is surprisingly difficult to discriminate between this prediction and that of Eq. (1) over a 3-log-unit intensity range. The existing data from the cited studies can be fitted with either function within close to the experimental error. Only by extending the data for another decade or two of intensity can a clear determination be made of the principle underlying visual dynamics.

The lower part of this range is precisely that obscured by rod-mediated response in previous studies, including those of Kelly,[7] who used white light and a very large (65°) field to test his theory, with no attempt to isolate responses for individual cone types. Addition of the rod response has the effect of increasing the absolute sensitivity at low intensities. While there should not be a smooth transition between rod- and cone-mediated response regions, a survey of CFF every half-decade of intensity might well obscure the transition cusp and give an adequate fit to the square-root prediction, based on the contamination by rod responses. The present studies provide a critical test of the Kelly–Veringa solution to the diffusion equation (viz., the square-root law) as a predictor of isolated cone responses.

B. Linearity and the Time Constant of the Linear Response

It is now well established[4,7,15,19] that the performance of the visual system is linear close to the CFF point (for modulation depths near 100%). The concept of linearity is used here in the sense of threshold at any intensity level being determined solely by the modulation amplitude of the stimulus and is unaffected by changes in its mean intensity. In contrast to this behavior, adaptive variation in threshold obeying Weber's law with variation in mean intensity would require a multiplicative nonlinearity.

If the visual system were truly linear near the CFF point, then the linearity implies that light adaptation would have no effect on the form of the response. The CFF/intensity function would therefore represent the system response under fully dark-adapted conditions. The present experiments may therefore be regarded as providing a full-range specification of the dark-adapted response of the cone system under investigation

C. Animal Studies

The CFF/intensity function and the modulation envelope have been measured in several animal studies of individual receptor function. These data may therefore be used as a direct test of the Ferry–Porter function as a description of the photoreceptor response.

In limulus, which has only one receptor type, Pinter[10] measured the modulation envelope over a 3-decade range of intensities. The results are shown in Fig. 1B, on log intensity, linear frequency axes. On the assumption that the response amplitude is linear with stimulus modulation amplitude, the straight line shows the best fit of the Ferry–Porter function [Eq. (1)]. The function provides a good description of limulus photoreceptor dynamics.

Similar data from turtle retina are plotted in the same fashion in Fig. 1B for intracellular cone recordings[12] and for recordings from horizontal cells.[11] In the former study the frequency responses were obtained by Fourier transformation of impulse responses, rather than by direct measurement. In both cases the results are well described by the Ferry–Porter function over as much as a 5-decade range.

Based on a two-parameter fit of slope and intercept, the best-fitting square-root function to the full range of intracellular[12] data is shown as the dashed curve in Fig. 1B. The standard error of the fit is ±0.268 log Td, versus ±0.013 log

Td for the Ferry–Porter function (a ratio of 20.3 in favor of Ferry–Porter). Evidently Kelly's simplified solution to the diffusion equation is a poor description of receptor phototransduction behavior in comparison with the fit of the Ferry–Porter law. Since phototransduction is similar at all phylogenetic levels, it would be surprising to find human cones exhibiting fundamentally different behavior. If psychophysical measurements of single receptor mechanisms were to show the square-root behavior to hold for human flicker responses, it would presumably be a postreceptoral phenomenon.[20] If, on the other hand, Kelly's data result from the combination of responses from more than one receptor type, the psychophysical responses mediated by a single receptor may conform more closely to the Ferry–Porter behavior and hence reflect the underlying receptor dynamics. Our study is designed to clarify this link between human psychophysics and individual receptor responses.

2. METHODS

A. Stimuli

The basic stimuli and procedures were the same as used in the previous study in this series, with variations to be described here. For the main experiments the test stimulus consisted of a diffused array of 25 light-emitting diodes (LED's) with a dominant wavelength of 660 nm. Control experiments were conducted with a set of LED's filtered to produce light with a dominant wavelength of 505 nm. These were actually 555-nm LED's viewed through a Wratten 47 gelatin filter, which strongly attenuates above 500 nm. Thus the luminance of the 555-nm LED's was attenuated by ~4 log units, but the residual transmitted light had a dominant wavelength of 505 nm, as determined by a spectroscopic match, and was still sufficiently bright to span the scotopic luminance range.

The stimulus event consisted of a burst of sinusoidal or square-wave flicker modulation presented with a gradual onset and offset in the form of a cosine envelope of 1-sec duration (Fig. 2, inset), so that flicker could not be detected by transients at the beginning or end of the presentation. The degree to which such transients were reduced can be expressed in terms of the bandwidth of the stimulus in the Fourier-transform domain (Fig. 2). The frequency bandwidth of this envelope is 1 Hz at half-height, with sensitivity of the first sidelobe at −32 dB and −18-dB/octave attenuation thereafter. Note that Fig. 2 has a highly compressed vertical axis expressing a range of 8 log units from top to bottom.

The solid straight line in Fig. 2 represents the fall in visual sensitivity with frequency, corresponding to the Ferry–Porter law data to be described in Section 3. This has a negligible slope in comparison with the steepness of the stimulus bandwidth. Thus the visual effect of the stimulus at the test frequency is approximately 30 times greater than at the first sidelobe, and the test frequency and must therefore completely dominate the threshold determination.

This analysis of the stimulus characteristics therefore demonstrates that the estimate of sensitivity to the test frequency is not distorted by aliasing introduced from the cosine modulation envelope. Moreover, when the envelope is of a fixed duration, the effects of both linear integration and probability summation are virtually independent for all modulation frequencies. A mathematical derivation of this independence is provided in Appendix C.

The other possible artifact in the use of a cosine window is that any type of static nonlinearity in either the LED intensity function or the phototransduction process could gener-

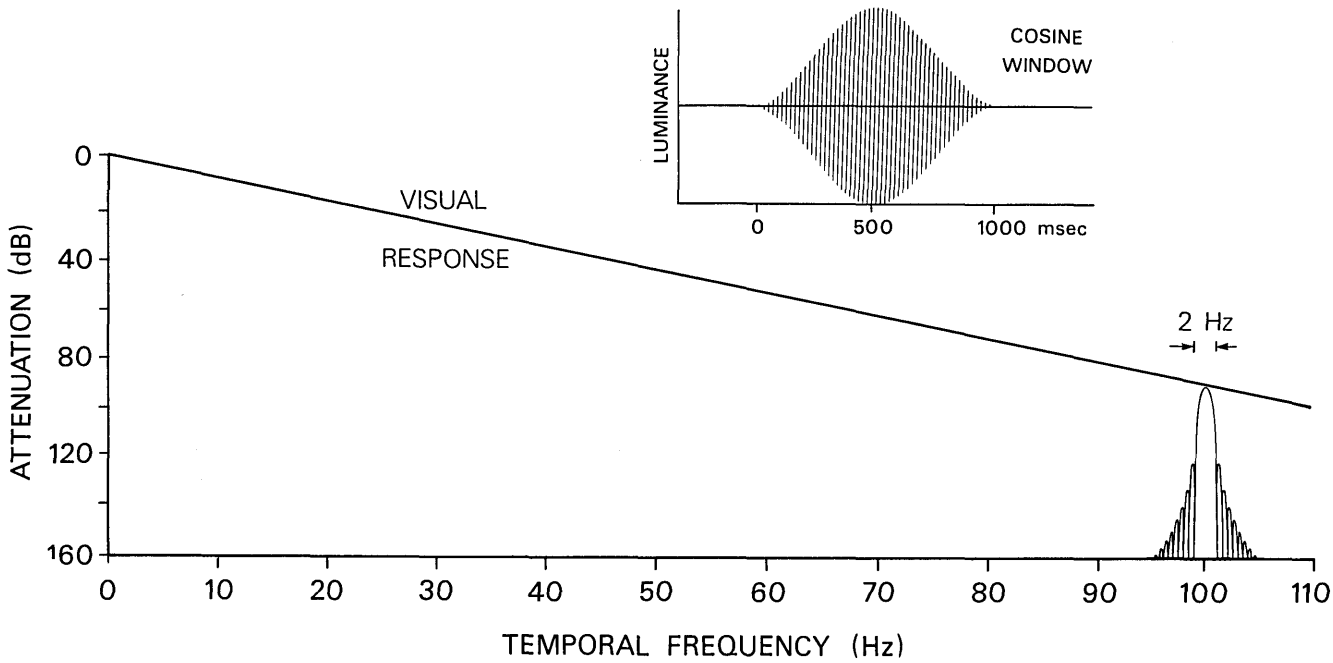

Fig. 2. Temporal characteristics of the stimulus used for this study. The inset depicts 100-Hz modulation around the mean intensity level with a cosine temporal envelope (100% Tukey window). The attenuation plot shows a frequency bandwidth of this window of ±1 Hz to first zero with an attenuation of −18 dB/octave around the test frequency. The straight line indicates attenuation of 100 dB over 100 Hz in visual sensitivity based on the Ferry–Porter function for periphery (see Section 3).

ate a distortion product resulting in an intensity shift that followed the slow time course of the cosine window itself. Such artifacts were perceptually absent when the LED intensity/current function was linearized by compensating the digital-to-analog output on the basis of calibration of the light output with a fast photodiode. The calibration curve was unaffected by output speed, being the same for 2-μsec pulses as for 1-sec steps. This linearity was checked regularly during the experimentation period. In fact, the observers could readily distinguish between the artifactual, 1-cycle intensity shift and the rapid flicker near CFF under all the present measurement conditions. The alternative tactic of using a suprafusional frequency to introduce an equivalent artifact into the blank stimulus in the two-alternative, forced-choice task was not adopted, because we wanted to keep the stimulus as pure as possible. If there had been an artifact, it was preferable to eliminate it rather than to force a discrimination with an artifactual intensity shift as a masking condition in both levels.

The 1-sec stimulus duration was designed to be sufficiently brief to minimize adaptation to flicker during the threshold determination. The two-alternative forced-choice staircase[21] presented stimulus or no stimulus of equal probability on each trial. The asymptotic level of the staircase gave the modulation frequency for which 75% correct performance was obtained. Three threshold estimates (or more where variability was larger) were averaged to estimate CFF under each condition tested (see Appendix A for full evaluation of the staircase procedure).

B. Procedure

The observers' pupils were dilated with 1% mydryacil to hold the aperture constant at all intensity levels, which were controlled by means of calibrated Wratten 96 neutral-density filters mounted in a light-tight mask worn over the eyes. One eye viewed the stimulus through the appropriate filter density, while the other was occluded and in darkness.

The spatial configuration of the presentations was designed to stimulate a retinal region that was as nearly uniform as possible. The foveolar region at the bottom of the foveal pit has only cone receptors of constant inner- and outer-segment diameters, outer-segment length, axon length, cone pedicle size, and connectivity.[14] The stimulus for central viewing was therefore chosen to be 0.5° in diameter to stimulate this homogeneous foveolar region. The peripheral stimulus was placed at 35° eccentricity on the horizontal temporal meridian, as this was the retinal region of highest flicker sensitivity in preliminary experiments. At this eccentricity the density of both cones and rods is approximately constant for a radius of at least 10° around any point, and the receptor morphology is also homogeneous.[13] For peripheral experiments an auxiliary LED was used to provide a fixation point. Fading of the peripheral stimulus was avoided by instructing the observers to shift fixation over a range of ~2° from the fixation point between trials.

C. Isolation of R Cones

The accepted technique to isolate the responses mediated by each separate cone type is to take advantage of their wavelength selectivity to stimulate the desired type in the test field, together with an adapting field of a different wavelength to desensitize the other receptor types.[22] Even in the form in which they are used, such methods face a number of unresolved problems, as discussed in Appendix B. In application to the present paradigm of the Ferry–Porter function, an insurmountable deficiency is that sensitivity is independent of mean intensity level in the region of CFF, as demonstrated in Subsection 2.G. This behavior contrasts with the nonlinear behavior of Weber's law, in which the incremental response decreases as intensity increases. The independence of sensitivity from background intensity near CFF implies that the response of competing cone systems in the CFF region cannot be suppressed by the use of a moderate adapting background. Conversely, if the background is increased sufficiently to produce adaptation, it will move the response out of the linear range that is intended as the subject of this investigation (see Appendix B).

Since the consequence of the linearity near CFF is that the traditional chromatic adaptation technique cannot be used for the present studies, a method with an entirely different theoretical basis from the conventional approach is required. The approach used here relies instead on two principles:

(i) CFF will be determined by the receptor type most sensitive to the test wavelength (R cones in the case of a 600-nm light). A preferential stimulation of ~1 log unit for the R versus the G cones is obtained simply by the use of the 660-nm light.[21,23]

(ii) The use of an equiluminant white surround will tend to suppress contamination from the responses of receptor types less sensitive to the test light by lateral inhibition into the test area. This principle is explained below and demonstrated for the rod system.

While an equiluminant surround actually slightly enhances flicker detection,[24] our surround was equiluminant only for the R cones. In terms of scotopic retinal illuminance, the surround was 3 log units more intense than was the 660-nm light for the rod system. As will be described in Section 3, we verified that this intensity difference made the stimulus invisible to the rods at all intensities used, and hence they could not contribute to the CFF/intensity function. The white surround was also ~1 log unit more intense for the G cones than was the 660-nm stimulus, based on the convolution of each stimulus spectrum with the spectral sensitivity of the two cone classes. For both the foveolar and peripheral conditions, the G-cone responses in the stimulus region should therefore also have been inactivated by the effects of lateral inhibition from the response to the white surround into the center, since the G cones are effectively viewing the stimulus in a deep black hole.

Prevailing evidence[25,26] suggests that the predominant component of lateral inhibition is cone specific. Thus R-cone responses in a central field will be inhibited by R-cone stimulation in a surround but not by G-cone stimulation in the surround.

This result makes it clear that the conditions for lateral induction are very different for the two cone systems. There should be essentially no inhibition of the R-cone response in the center, since it is at a higher intensity than the R-cone surround response. Conversely, the G-cone stimulation in the center is ~1 log unit lower than in the surround, a condition in which there is such strong lateral inhibition that

flicker sensitivity is proportionately reduced by 1 log unit for white-on-white stimuli in a central 0.5° fields.[24] Since we used foveal fields of this diameter, and proportionally scaled peripheral fields, the same should have been true for the G-cone response under our stimulus conditions. Thus the surround conditions alone should have been sufficient to ensure that the responses in the present study were mediated solely by R cones. We were thus able to isolate the R-cone response psychophysically and determine the validity of the Ferry–Porter law for the pathway mediated by a single receptor system.

3. RESULTS

A. Elimination of Rod Component

To set the stage, we first replicate the results of previous investigators under rod-favoring conditions. Pilot studies showed that the retinal region with the highest temporal sensitivity for the standard 5.7° field was at 35° eccentricity in the upper temporal field. We therefore selected this location for all peripheral experiments in the present study. At this location there are, according to Oesterberg,[13] approximately 100,000 rods and 4000 cones per square millimeter of retina. The relative receptor densities are therefore vastly in favor of the rod system, and a substantial scotopic limb would be expected in the CFF/intensity function.

To optimize the rod contribution, the test field was viewed with a dark surround, and the function was measured for test wavelengths of 660 and 505 nm. Both sets of data (Fig. 3A) show the expected scotopic limb for CFF versus log photopic luminance, leveling off at ~20 Hz. The photopic limb was beyond the range testable with the 505-nm source, since the luminance available with LED's is low at this wavelength. The scotopic limbs are separated by ~3 log units, as expected from the relative increase in rod sensitivity toward shorter wavelengths (open arrow, Fig. 3A).

We next added the white surround at a photopic luminance equal to that of the 660-nm stimulus. This surround luminance was 3.1 log units higher than the stimulus in terms of scotopic luminance, which would be expected to suppress rod function in the test field by lateral inhibitory interactions. The results (filled circles, Fig. 3B) show that the scotopic limb is now absent from the 660-nm data, which fall on a straight line over the entire visible luminance range.

To ensure that rod function was abolished, and that a remnant of the rod responses was not contaminating the lower end of the function either by residual sensitivity or by inhibition of the cone responses, we also tested the 505-nm condition with the white surround 3.1 log units higher in scotopic luminance. The stimulus was now always invisible (open circles, Fig. 3B), up to at least 3 log units above its previous threshold. Thus it is most unlikely that rod responses were affecting the photopic data at 660 nm. We therefore consider that the 660-nm condition with a photopically equiluminant surround is sufficient to isolate peripheral R-cone responses for the entire luminance range.

B. Validation of the Ferry–Porter Law for Isolated R-Cone Stimulation

Having established the isolation of the R-cone response, we may compare the Ferry–Porter description with that of the diffusion hypothesis for the most homogeneous element of the neural pathway available to psychophysical investigation. Square-wave temporal modulation was used, both to provide a slight increase in the effective modulation amplitude and to permit direct comparison with earlier studies. The field conditions were the same as for Fig. 3, a 5.7° field at 35° eccentricity. Data for two further observers are presented in Fig. 4, with CFF values being measurable over

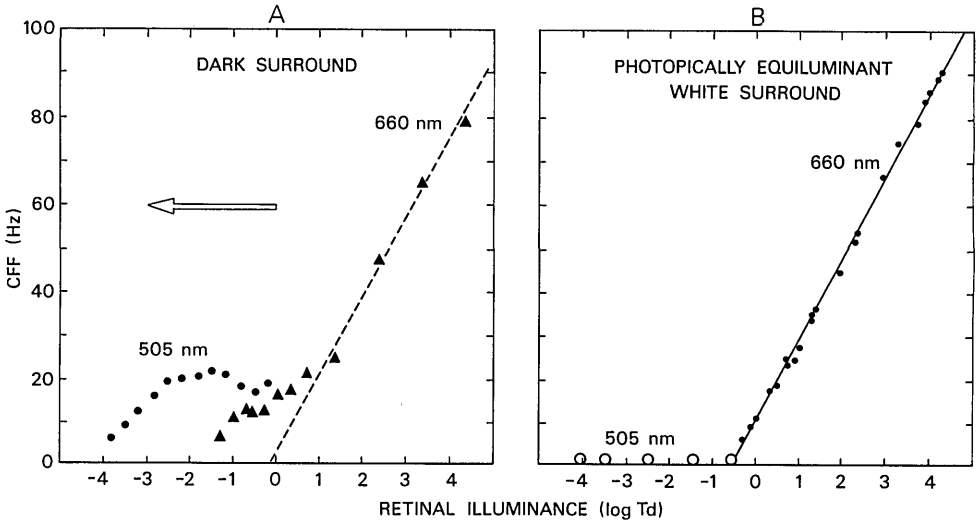

Fig. 3. A, Shift of the rod-mediated limb of the psychophysical CFF intensity function with test field wavelength. Data were measured by a forced-choice technique for a 5.7° field at 35° eccentricity on the horizontal temporal meridian. The stimulus was 100% sinusoidal modulation of a LED array. Circles, test field at 505-nm dominant wavelength with dark surround; triangles, test field at 660 nm with dark surround; horizontal arrow, shift of scotopic threshold expected on the basis of the CIE scotopic luminosity function. Observer RDH. B, CFF/intensity function with a white surround for the same observer. Filled circles, test field at 660 nm with photopically equiluminant hemispheric white surround; open circles, absence of scotopic detection for a test field of 505 nm with a white surround at 3.0 log units higher scotopic luminance. This combination matched the scotopic effect of a photopically equiluminant surround at 660 nm. Average standard errors of the means in this and other figures are less than the size of the symbols.

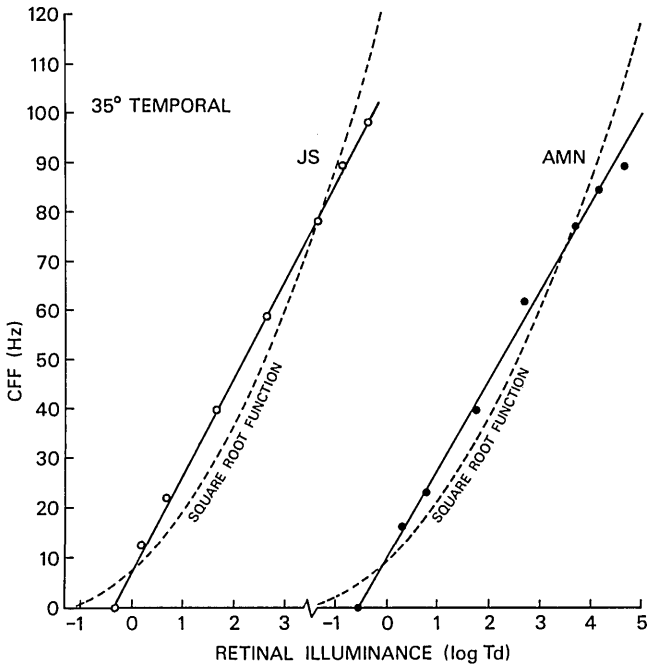

Fig. 4. Ferry–Porter law for two other observers at 660 nm under same field conditions as for Fig. 3B but with 100% square-wave modulation. Note the tight adherence to the best-fitting Ferry–Porter functions (straight lines) and departure from the best-fitting square-root functions (dashed curves).

approximately a 5-log-unit range. The solid curves show the best-fitting Ferry–Porter functions, with slopes of 19.5 and 18 Hz/decade and correlations in the range of ≥0.999 for both observers. The dashed curves show the best-fitting square-root functions. Clearly the square-root functions do not provide a good description of the psychophysical sensitivity for isolated R-cone stimulation.

C. Statistical Analysis

A more quantitative evaluation of the fit to the two hypotheses may be obtained by least-squares regression of each CFF function onto the data. These amount to two-parameter fits of Eq. (2) with exponents of $P = 1.0$ (Ferry–Porter) or $P = 0.5$ (diffusion equation). Another possibility is a three-parameter fit of Eq. (2) with a variable exponent to ensure that the better fit of the two is close to the best possible fit when P is completely free to vary.

The results of the regression analysis clearly favor the Ferry–Porter solution. The residual error variance with a fixed exponent of 1.0 was only ±0.112 Hz. For the 0.5 exponent, the error variance increased by more than a factor of 5 to the level of ±0.58 Hz. This difference may be analyzed statistically by means of the χ^2 test. If s_e^2 is the smaller error variance and $s'_e{}^2$ is the greater, then the F ratio for a significant difference in the fits[27] is given by

$$F = (s'_e{}^2 - s_e^2)(n - 1). \quad (3)$$

Application of the formula results in an F ratio of $F = 182$, which represents a better fit for the Ferry–Porter function far exceeding a significance level of $p < 0.01$.

Having answered the question of which fixed-exponent model provides the better fit to the data, we turn to the second question of how closely the models compare with a three-parameter fit in which the exponent of Eq. (2) can freely vary. The least-squares minimization resulted in an exponent of 0.997 with an error variance of ±0.111 Hz; both of these values are close to those for the Ferry–Porter model. In fact, application of the F test for error variance results in a value of $F = 0.35$, which is well below significance for a difference between the two- and three-parameter models. Conversely, the F ratio for improvement of the three-parameter fit with the exponent of 0.997 over the diffusion model with a fixed exponent of 0.5 is $F = 180$, which again far exceeds the criterion level for $p < 0.01$. Thus the statistical analysis falls heavily in favor of the Ferry–Porter function as the best descriptor of the data, differing only at the third decimal place from a function with a freely varying exponent.

An alternative approach to the statistical analysis is to regress the functions with intensity as the dependent variable for the regression onto the frequency axis. Linear regression may then be performed with the use of either a linear or a square-root frequency axis. In both cases the regression will have the same variance properties because the residual error is calculated on the common luminance axis. The residual error (in terms of its standard deviation) for the Ferry–Porter function was ±0.055 log Td for the data from observer RDH in Fig. 3B and ±0.045 and ±0.133 log Td, respectively, for observers JS and AMN in Fig. 4. The residual errors for the square-root function fits were ±0.214, ±0.178, and ±0.249 log Td for the same three data sets. The F ratios of the variances from Eq. (3), by which the Ferry–Porter fit was an improvement over the square-root fit, were 254, 88.2, and 15.3, respectively, which are all again strongly statistically significant at $p \ll 0.01$.

D. Field Size

We next address the question of spatial summation. The field size and eccentricity conditions for Fig. 2B were chosen to provide stimulation of a retinal region homogeneous in terms of receptor morphology and receptive-field dimensions at all levels of the visual system. However, the result was to choose a relatively small field compared with the 65° field for which Kelly[7] obtained data conforming to a square-root function. To rule out field size as a factor in the difference between the CFF/intensity functions, we repeated the experiment, using 16°-, 2°-, and 0.5°-diameter fields centered at the same 35° location.

The results of varying field size are shown with linear CFF/log intensity axes in Fig. 5. All four data sets again fall on straight lines of the same slope throughout the available intensity range, suggesting that use of a large field *per se* is not the factor that produced Kelly's[7] results. The temporal response characteristic can therefore be said to remain unaffected by more than a 1000-fold variation in stimulus area.

A second consideration to which field size is relevant is whether the occurrence of lateral inhibition or spatial summation within the field is in some way responsible for the CFF/intensity characteristic. The 16° field covers 8 mm^2 on the human retina and therefore stimulates ~50,000 cones at the 35° eccentricity used.[13] Restricting the stimulus to 0.5° diameter reduces the field area by a factor of 1000, which should now stimulate only ~50 cones, and falls well within the summation range of the psychophysical "perceptive

fields" at this eccentricity.[28] Use of the equiluminant white surround should ensure that the small-field data are not contaminated by detection of flicker from stray light in retinal regions outside the test field. The response dynamics with such a small field should therefore be dominated by the excitatory response within the neurons representing that field at each level of the visual pathway and should result in minimization of the effects of areal summation.

The reduction in field size resulted in a substantial loss in sensitivity, represented by the 2-log-unit rightward shift of the data compared with the largest field size. Decreasing the field diameter from 2.0° to 0.5° decreases the area by a factor of 16 and the sensitivity by a factor of 10, which is approaching linear areal summation (Ricco's law). By contrast, the areal decrease between the 16° and 2° field sizes is a factor of 64 but produces approximately the same decrease in sensitivity of a factor of 10, corresponding approximately to Piper's law of square-root summation (exact correspondence would predict a sensitivity reduction by a factor of 8, compared with 64 for linear summation).

While reviewing the applicability of various laws, it is worth noting that the data of Fig. 5 are broadly incompatible with the Granit–Harper law [CFF = $k \times$ log area (Ref. 29)], since the value of k is not constant for the present data but varies between 1 and 0.5 (linear and square-root areal summation). The Granit–Harper law could be compatible with either Ricco's law or Piper's law but not both, as determined by the value of k.

E. Retinal Location

It has been suggested[30] that the speed of the retinal response increases with eccentricity. If such an increase occurs uniformly for all aspects of the response, then the CFF at each intensity should be higher in the peripheral location than in the fovea, and the slope of the CFF/intensity function should be steeper. (For example, if the time constants of all aspects of the retinal response were halved, then the CFF at each intensity should be doubled, with a resultant doubling of the slope.) This prediction is at variance with the classical data on the subject,[8,31,32] which tend to show a shallower slope for the photopic function in the periphery. However, these data are heavily contaminated by rod contributions, and moreover were obtained by an adjustment method that involved substantial adaptation to the flickering field before the threshold setting.

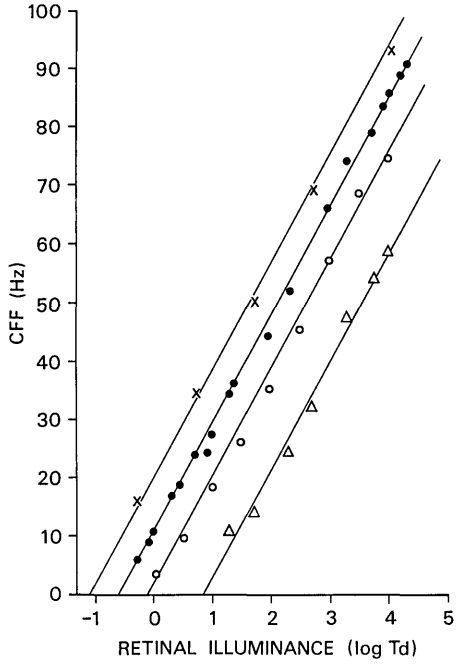

Fig. 5. Effect of field size on the photopic CFF/intensity function for 660 nm at 35° eccentricity. Filled circles, 5.7° data replotted from Fig. 3B; crosses, 16° field; open circles, 2° field; triangles, 0.5° field. Note the adherence to the Ferry–Porter law at all four field sizes, with a constant slope of 19 Hz/decade. Observer RDH.

The peripheral data presented in Figs. 3–5 have slopes of ~19 Hz/decade, far higher than the typical foveal values of ~12 in most previous studies. Since our data were obtained under conditions of rod exclusion and minimal flicker adaptation, they represent the isolated and unadapted temporal response mediated by the peripheral R-cone system. With these data as a baseline, we may now ask whether the slope difference is attributable to the difference in our psychophysical procedure or whether foveal responses tested under the present conditions bear out the predicted increase in time constant (reduction in slope) implied by the previous data.[30]

For this experiment, a central field of 0.5° was selected to stimulate only the foveola, in which the cones are of uniform diameter and length and the rods are completely absent.[14] Approximately 3000 cones are present within this area, which also represents a region of high uniformity with respect to the magnification of ganglion cell receptive fields.[9] The stimulus again had a hemispheric white surround of equal luminance to the test field to eliminate contamination from neighboring retinal regions and was in fact identical to the 0.5° field used for the small-field study of Fig. 5. To investigate the effect of field size in the foveola, the function was also measured for a field 0.05° (3 min) in diameter by viewing the same stimulus at a distance of 286.5 cm. This condition was designed to stimulate the central bouquet of ~30 cones in the foveola, within the limitations of fixation accuracy.

The CFF/intensity function for the foveola (Fig. 6, filled circles) again adheres to the Ferry–Porter law over a 4-decade range of intensity, with no evidence of rod contamination at lower intensities. There is a slight tendency toward a leveling of the function at the highest intensities. Below this level, the data fall on a straight line with a slope of 10.5 Hz/decade, approximately half the value for the peripheral data from the same observer. The same function provides a good fit to the data for the central bouquet (points) with a shift corresponding to a 1.2-log-unit decrease in sensitivity, in approximate correspondence with Piper's law, since the area has been decreased by 2 log units.

It is interesting to compare the sensitivity of the foveola with that at 35° eccentricity, since the two sets of stimuli should project to similar numbers of cones. The best-fitting peripheral functions for 5.7° and 0.5° are plotted as the dashed and dotted lines, respectively, in Fig. 6, showing that the functions converge to very similar asymptotic values of absolute threshold when similar numbers of receptors are stimulated at the two eccentricities. This comparison also emphasizes the radical increase in the slope of the Ferry–Porter law from fovea to periphery.

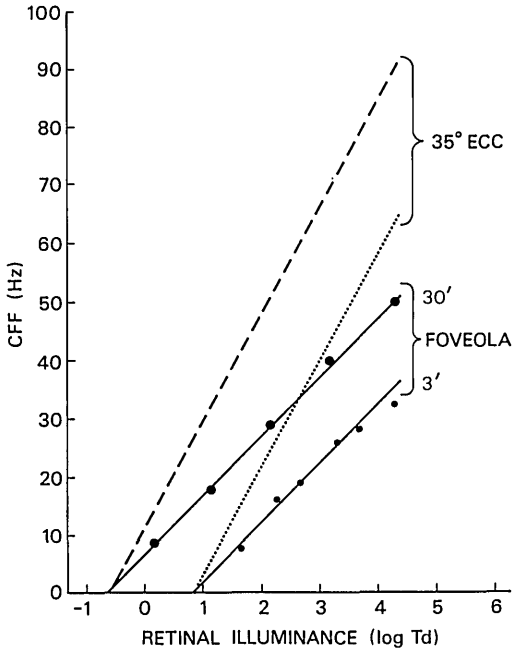

Fig. 6. Photopic CFF/intensity functions in the foveola. Test field at 660 nm with an equiluminant white surround. Large filled circles, 0.5° field; small filled circles, 0.05° field. Note the adherence to the Ferry–Porter law for both field sizes with constant slope of 10 Hz/decade. Dashed and dotted lines, best-fitting Ferry–Porter functions for 5.7° and 0.5°, respectively, at 35° eccentricity from Fig. 5, showing that the absolute threshold is the same at both eccentricities despite the change in slope of the functions. For observer RDH.

In some respects, the foveolar results differ from those in a recent report obtained with many of the same experimental controls and a forced-choice procedure.[33] In that study, CFF for long-wavelength flicker tended to saturate beyond ~3 log Td, rather than continuing to increase up to ~4 log Td as we have found. There are several methodological differences to account for the discrepancy. Their maximum modulation amplitude was only 60%, and may not have been so securely in the high-frequency linear response range. Their modulation envelope was a fixed number of cycles, which means that stimulus energy is reduced as frequency is increased, while it remains constant in the present experiments (Appendix C). (For example, their duration at $1/e$ height was 250 msec at 24 Hz but only 125 msec at 48 Hz.) Their equiluminant surround was also equichromatic, which does not act as such an effective isolator of the R-cone response because it has no basis for preferential inhibition of the G-cone response to long-wavelength flickering field by the white surround. Finally, their field size was 1.2° centered on the fovea, which we do not regard as stimulating a homogeneous retinal region (see Section 2). In fact, pilot data that are not otherwise relevant for the present study show that use of larger fields results in CFF/intensity functions that depart from straight lines, which may be attributable to the interactions between mechanisms with different temporal properties in different retinal regions. In conclusion, these discrepancies underline the concept that only when all factors are optimized for the isolation of separate and homogeneous cone contributions will unitary functions be obtained.

F. Spatial Frequency

Kelly[34] has made the suggestion that the changes in temporal response with eccentricity, such as those depicted in Fig. 6, might be specific to uniform field stimuli and be absent for grating stimuli of high spatial frequency. This suggestion is called into question by the small-field data of Fig. 6, which emphasize the higher-spatial-frequency components by virtue of the small fields but show the same change of slope with eccentricity as the large fields. A more direct test is to repeat the experiment with grating stimuli instead of uniform test fields.

The stimuli were constructed by modulating alternate rows of the LED arrays in counterphase (see inset, Fig. 7), using the same diffusing aperture as for the previous experiments. As a result of the projection geometry of the LED lenses, this arrangement gave almost uniform diffusion of the light from one LED to the next along the rows but almost no diffusion between rows (as determined photometrically with a Pritchard spectra-spot photometer). Viewed at the standard distance of 28.5 cm, these stimuli constrained the fundamental spatial frequency of modulation to 0.5 c/deg for the 5.7° field, which was presented at 35° eccentricity. For a 0.3° foveolar stimulus the same LED array was fixated from a distance of 573 cm by means of a front-surface mirror, resulting in a fundamental spatial frequency of 10 c/deg. The spatial frequencies of 0.5 and 10 cycles/deg are at equivalent points on the spatial frequency tunings for the two eccentricities.[35,36] They are also sufficiently high that they show no evidence of lateral inhibition in controlling the spatiotemporal sensitivity.[37]

Figure 7 shows that the grating modulation experiment gives a very similar picture to those for uniform fields. The data fall on the straight lines predicted by the Ferry–Porter

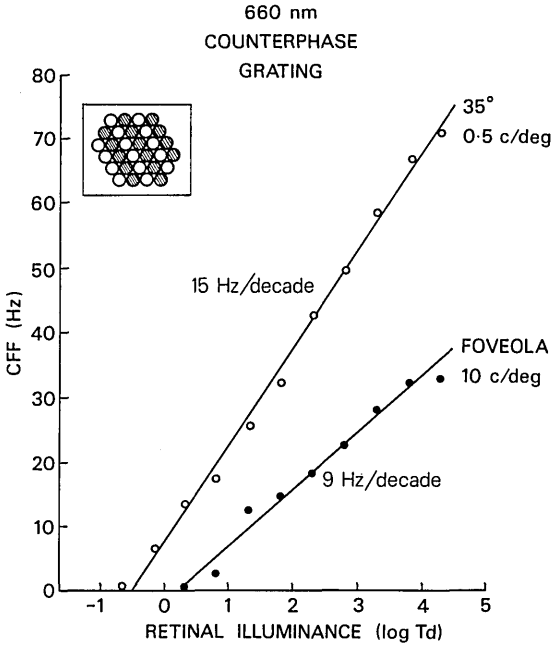

Fig. 7. CFF/intensity functions for counterphase spatial modulation at high spatial frequencies. Filled circles, 10-c/deg stimulus of 0.5° diameter in the foveola; open circles, 0.5-c/deg stimulus of 5.7° diameter at 35° eccentricity. Note the overall similarity to corresponding uniform field data of Figs. 5 and 6. Observer RDH.

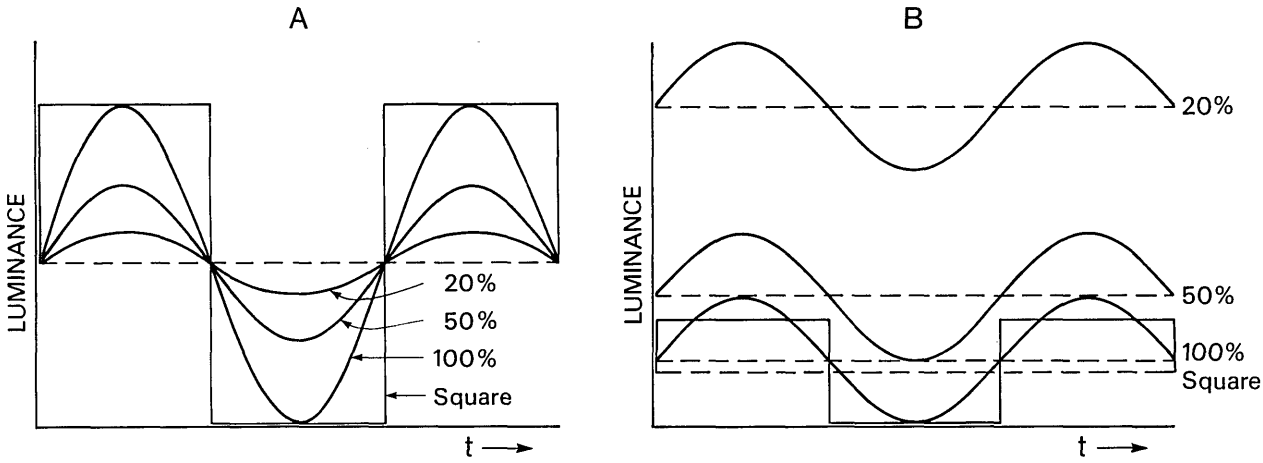

Fig. 8. Stimulus conditions for the test of linearity in the CFF region. A, Sinusoidal and square-wave modulation around a fixed luminance level. B, Rescaling of intensity (luminance) to obtain the same modulation amplitude for each stimulus in A. In the case of the square wave, this is the amplitude of the Fourier fundamental frequency.

law except for a slight decline at the highest intensities and meet at approximately the same threshold values at the two eccentricities. The slope for the 35° eccentricity function is substantially steeper than for the foveolar data. These data therefore confirm that the characteristics observed for uniform field responses apply equally to stimuli of high spatial frequency (relative to the visible range at each retinal location). Since high spatial frequencies are mediated by the receptive-field centers, this observation eliminates any involvement of lateral inhibition in the variations of response behavior with retinal locus.

G. Linearity

The final question that we address is the linearity of the temporal response in the high-frequency region close to CFF. Both Ives[4] and de Lange[38] obtained data supporting the hypothesis that the CFF is mediated by the fundamental Fourier component of the stimulus waveform, since higher harmonics are necessarily above the CFF and are therefore sufficiently attenuated that they do not contribute to its determination. Moreover, Kelly[16] has suggested that the response behavior in the CFF region is linear, in the sense that it is independent of mean adaptation level, and is determined solely by the modulated portion of the stimulus. Thus a 20% modulation at a mean luminance of 100 cd/m^2 should produce the same CFF value as 100% modulation at 20 cd/m^2, since the modulated component varies by 20 cd/m^2 in each case (see Fig. 8B). This question has not been addressed for isolated cone system responses. We therefore measured CFF/intensity functions for the 5.7° field at 35° eccentricity with the equiluminant white surround under a range of modulation conditions. These were 20%, 50%, and 100% sinusoidal modulation and 100% square-wave modulation (with a Fourier fundamental of 127%), as shown in Fig. 8. The data are presented in terms of CFF as a function of mean intensity of the stimulus in Fig. 9A (corresponding to the equivalence conditions shown in Fig. 8A). There is a progressive increase in the position of the CFF/intensity function as modulation of the Fourier fundamental is increased from 20% to 127%. Note that for the upper two curves the stimulus has the same peak-to-peak amplitude of 100%.

To show whether this increase is proportional to modulation amplitude, the data are replotted in Fig. 9B as a function of the absolute amplitude of modulation, as depicted in Fig. 8B. They now all coincide on a single straight line, indicating that modulation amplitude is the factor that governs the CFF behavior, regardless of the mean intensity of the stimulus. As Kelly[16] has shown, this is contrary to the behavior at low temporal frequencies, where the threshold modulation varies directly with mean intensity, in a manner consistent with Weber's law.

The solid line in Fig. 9B shows the exponential function of the Ferry–Porter law [Eq. (1)], which provides a close fit to the data at all modulation amplitudes. The fact that the data coincide when plotted in terms of the Fourier fundamental confirms and extends over a 5-decade range the results of Ives[4] and de Lange,[38] who showed that the fundamental Fourier component of the stimulus governs the high-frequency behavior of the visual response. These data further confirm Kelly's[18] suggestion that the high-frequency response is controlled solely by modulation amplitude and is independent of mean intensity level.

4. DISCUSSION

A. Wide Jurisdiction of the Ferry–Porter Law

The experimental conditions were designed to isolate the responses of a single cone class at homogeneous retinal loci. The results are uniform in validating the Ferry–Porter formulation of the CFF/intensity relation [Eq. (1)] over more than a 5-decade intensity range and a wide variety of stimulus conditions. Although both the time constant and the threshold constant may vary, the logarithmic relation between CFF and intensity holds for fovea and periphery, for uniform fields projecting to between 30 and 100,000 cones, for high-spatial-frequency gratings, and for modulation amplitudes from 20% to 127%. The Ferry–Porter law may therefore be regarded as the operating principle that sets the frequency limits on temporal dynamics throughout the useful range of photopic vision. Modulation sensitivity (below

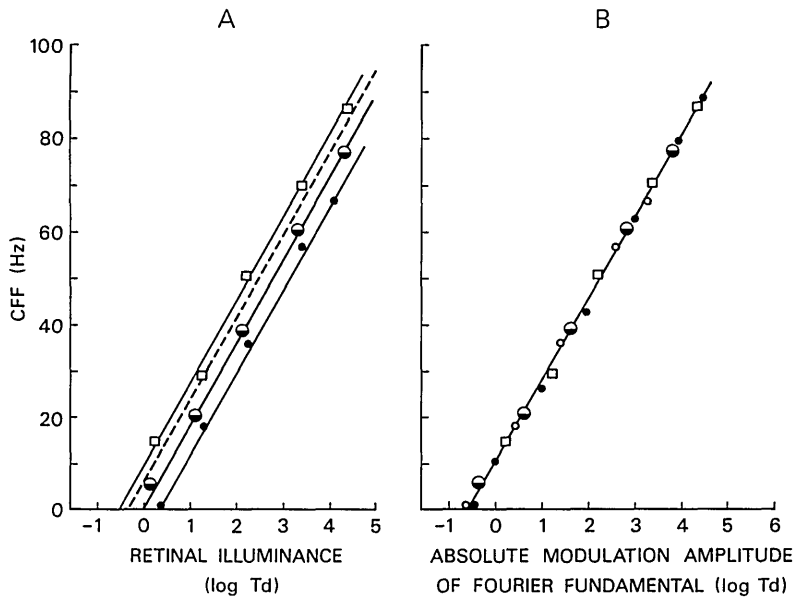

Fig. 9. Linearity of the peripheral CFF/intensity functions with waveform and modulation depth with same field conditions as Fig. 3B. Filled circles, 20% sinusoid; half-filled circles, 50% sinusoid; open circles, 100% sinusoid (omitted in A for clarity but represented by a dashed line); open squares, 127% square wave. A, Data plotted with respect to mean stimulus intensity. B, Data plotted with intensity scaled in terms of absolute amplitude of the fundamental Fourier component (see Fig. 8). For observer RDH.

~20% modulation) is governed by other principles and is not included in this generalization.

B. Implications of Linear High-Frequency Behavior

Figure 9 demonstrates that the response behavior in the CFF region is linear, in the sense that it is independent of mean adaptation level, and is determined solely by the modulated portion of the stimulus. Since these data involve measurement of sensitivity in relation to both modulation and frequency, the same data may be regarded as defining the temporal characteristics of the linear mechanism involved in the detection of high-frequency flicker. This linear mechanism must precede the nonlinear process corresponding to Weber's law, since the information lost by response compression at lower frequencies could not be later extracted from below the noise level by a compensatory gain increase at a later stage. Since Weber's law behavior has been demonstrated to occur in the receptors themselves,[39] the linear-response characteristic must be also determined in the receptors if it is to precede the nonlinear behavior.

Given its importance in setting the limits on all further visual processing, the linear temporal response should be characterized in greater detail. (Although in principle the measurements of this response may be distorted by postreceptoral filtering, we shall make the assumption, on the basis of the similarity to receptor responses discussed in Section 1, that the psychophysical response measured under linear conditions is solely determined by the receptors.) Kelly[7,15] has argued that the linear, or unadapted, frequency response cannot be close to the Ferry–Porter law because it would violate the Paley–Wiener criterion for the existence of a physical (i.e., causal) impulse response corresponding to the frequency response. As is shown in Appendix D, we consider that the Paley–Wiener criterion is a mathematical formalism not applicable to physical systems and is therefore irrelevant to the question.

The classical approach to performing the inverse Fourier transform of a frequency response function in the absence of phase information is to fit the candidate function with a set of functions whose responses are known for both the time and the frequency domains, viz., single-pole filters. Although the solution is multiply determined, it does permit the demonstration that a solution exists for a particular frequency function within the experimental error.

In Fig. 10A the axes of Fig. 9B are rotated to express the data in the form of a frequency response characteristic by plotting log absolute modulation sensitivity as a function of log frequency, which again illustrates that the thresholds are independent of mean intensity of the stimulus over this range. The figure emphasizes the steep frequency attenuation obtained by the visual response at high frequencies, reaching a slope of at least −8 (160 dB per decade). As a simple possibility, the best-fitting 8-pole filter function with equal time constants for each pole is shown as the solid curve running through the data. It provides an adequate fit to the data, although there is still room for improvement, corresponding to the minor discrepancies between this function and the Ferry–Porter function (which fit the same data almost perfectly in Fig. 9B). This fit serves as a demonstration that the Ferry–Porter function corresponds closely with a physically realizable description of the linear response of the retina (*vide* Figs. 1–7) over the full measurable range of intensities.

The best-fitting square-root function is also shown (as the dashed curve), but it does not give a good account of the frequency response mediated by a single receptor type, with deviations of as much as 1 log unit at low frequencies and 0.5 log unit in the other direction in the mid frequencies. We conclude that the linear, excitatory response of the visual system for isolated R-cone stimulation has a monotonically decreasing frequency response approximating an 8-pole discrete filter characteristic.

The impulse response of the same 8-pole filter, shown in Fig. 10B, corresponds to the predicted form of the linear, dark-adapted receptor response to a brief flash. It has all the typical features of the receptor responses from which Fig. 1B was derived. These include an apparent delay before any measurable response is obtained, an accelerating ascent toward the peak at 50 msec for this peripheral site, and approximate symmetry around this peak, except for the trailing edge, which declines more gradually. This equivalence is hardly surprising, since Baylor *et al.*[39] chose a similar multipole filter model to fit their recorded receptor responses.

C. Incommensurability of Foveal and Peripheral Results

The data of Figs. 5 and 6 showed the substantial difference in slope of the CFF/intensity function as eccentricity is varied. This implies that no fixed compensation of the intensity can bring the foveolar data into line with the peripheral data at all intensity levels, as has recently been claimed by Raninen and Rovamo.[40] In fact, the absolute intensity thresholds (x intercepts) are themselves equated by the field sizes selected for the experiment. Thus at absolute threshold no further intensity compensation would be desirable, while an intensity reduction of more than 2 log units is required at 35° to obtain a match with the foveolar CFF of 50 Hz at the highest intensity tested. This suggests that the difference in CFF from foveola to periphery at high intensity cannot be due to a difference in absolute sensitivity. Only a rescaling of the frequency axes could bring the foveolar and peripheral data into alignment. The absence of differences in absolute sensitivity appears to invalidate the utility of the compensation for total luminous flux (F scaling) proposed by Raninen and Rovamo. Instead, the difference is entirely attributable to a difference in temporal processing between the two retinal regions.

A further point to be made from these data is the comparison with previous research that used different psychophysical techniques. For a fixed field size of 0.5° in both foveola and periphery, the CFF values in Fig. 6 are equal (33 Hz) only at 500 Td. For lower intensities the data conform to previous results[8,9,32,41] in showing a lower CFF in peripheral observation, but for higher intensities the effect is in the reverse direction. By 50,000 Td the peripheral CFF for this tiny field reaches 65 Hz, while the foveal value is only 49 Hz. Thus the variation of CFF with eccentricity depends heavily on the intensity level at which the experiment is conducted. We consider that the variations are best characterized in terms of the log slope and the intercept of the CFF/intensity function, which are related to the time constant and the absolute threshold, respectively, of the linear mechanisms at each retinal location.

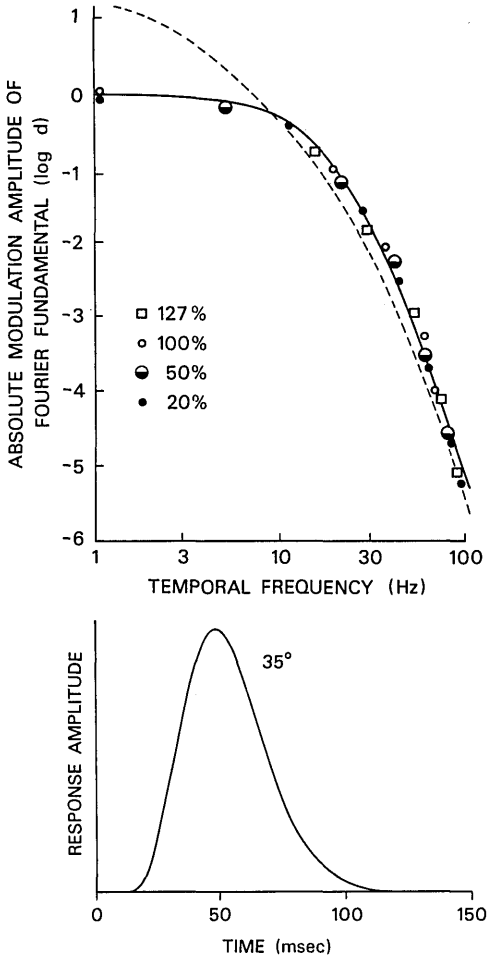

Fig. 10. A, Data of Fig. 8B replotted as a modulation sensitivity function, in terms of reciprocal of amplitude as a function of temporal frequency at CFF, in double logarithmic coordinates. This plot illustrates the temporal frequency tuning of the linear visual response at this eccentricity (35°). Solid curve, best-fitting 8-pole filter function; dashed curve, best-fitting square-root function. B, Impulse response of the 8-pole filter.

D. High-Spatial-Frequency Responses

Figure 7 shows that the grating modulation experiment gives a very similar picture to those for uniform fields. The data fall on the straight lines predicted by the Ferry–Porter law, except for a slight decline at the highest intensities, and meet at nearly the same threshold values at the two eccentricities. The slope for the 35° eccentricity function is substantially steeper than for the foveolar data. These data therefore confirm that the general characteristics observed for uniform field responses apply equally to stimuli of high spatial frequency (relative to the visible range at each retinal location). Since high spatial frequencies are mediated by the receptive-field centers, this observation minimizes the possibility of involvement of lateral inhibition in the variations of response behavior with retinal locus.

On the other hand, these high-spatial-frequency conditions did not result in identical responses to the uniform field data of Figs. 5 and 6. The peripheral slope has dropped by ~25% to 15 Hz/decade, and the foveolar slope is reduced by ~10%. This may be regarded as preliminary evidence that the speed of the linear visual response is slightly slower at high than at low spatial frequencies, particularly in peripheral vision. Such differences would be counter to the conclusion of a previous study of temporal integration for gratings,[27] but the differences are too small to be discriminated by the temporal integration method. Since the same cone population mediates all spatial frequencies, the temporal differences must be attributed to postreceptoral processing, possibly by a difference in conduction velocity between the magnocellular and parvocellular systems.[42]

E. Conclusion

The original inspiration for these studies was to narrow the gap between retinal physiology and psychophysics by designing experiments feasible for both modes of investigation. From the psychophysical perspective, this involved testing between hypotheses developed for overall visual function in a psychophysical paradigm optimized for stimulating an isolated receptor pathway. Instead of providing a purely descriptive formulation of visual behavior, the most adequate hypothesis may then be said to characterize the function of an elemental unit of the visual system. To the extent that this unit corresponds to one whose function is measurable physiologically, the functional properties may then be compared directly between the two levels of study.

While only psychophysical experiments were conducted in the present study, progress was made toward the goal of connecting the two modes. Receptor responses from previous research were found to conform more closely to the Ferry–Porter law than to a square-root function, in an apparent discrepancy from the claim[7] that human psychophysics conform better to the square-root function. The present results resolve this discrepancy by showing that, for psychophysical conditions more closely approximating those of the physiological studies, the results now comply with the same Ferry–Porter law. This resolution provides a firm basis for continuation of the conjunction between the two fields of study. It is to be hoped that retinal physiologists will also attempt to use conditions conducive to comparison between the two fields, bearing in mind the inherent limitations of psychophysics.

APPENDIX A: PSYCHOPHYSICAL STAIRCASE PROCEDURE

Staircase Algorithm

A pragmatic adaptive staircase procedure was developed to obtain rapid convergence of the staircase to the asymptotic threshold level. It holds the observer criterion and response bias within predefined limits. The principle of the pragmatic adaptive staircase is to use the average percentage of correct responses over all preceding trials at the current stimulus level to determine whether to change the stimulus on the next trial. In this application the stimuli were varied in 2.5-Hz steps of frequency or 0.1-log-unit steps of modulation amplitude. The percent correct at the current stimulus level (frequency or modulation) is summed with those of the two adjacent levels for the determination of the current percent correct to provide extra stability in the estimation in the region of the maximum likelihood for threshold determination. This percent correct is then compared with the desired 75% correct level of performance, and the stimulus is either increased or decreased by one step with a probability of 50% in the direction appropriate to reach the 75% level.

The slope of the psychometric function is not determined in this algorithm, and no slope value is assumed. The only assumption is that the psychometric function is sufficiently linear around the 80% range that the mean for the adjacent steps is close to that of the current level, so that averaging does not cause significant distortion.

The decision that threshold has been reached is made not on the basis of reversals in the staircase but on meeting three separate performance criteria. For the latest 15 trials in the sequence, the staircase is terminated if the following conditions are met:

(1) The slope of the staircase values over time is zero (±1 step per 15 trials),
(2) The percent correct is 75% ± 10%,
(3) The YES/NO bias equals the ratio of stimulus occurrences ±10%.

Five trials at the beginning of the sequence are included in the cumulative probabilities to improve stability but are not used in the testing sequence of 15 trials. Thus the minimum possible run length is 5 + 15 = 20 trials. The run continues until the latest sequence in the staircase passes all three tests, when it is assumed that threshold has been attained, and the run is terminated.

Operation of the Staircase

The most important feature of the procedure was that the performance reached a stable level, forming a flat function at the end of the staircase sequence. Any tendency of the sequence to slope up or down was regarded as an indication that the stimulus values were not at a stable threshold level, and thus the staircase continued.

The percent-correct criterion was included to control against differences in the detection criterion employed by different subjects. Although the two-alternative, forced-choice procedure controls the guessing rate at 50%, it is still possible for subjects to differ in the range over which the criterion varies during the threshold estimation procedure. If the variation is large, it has the effect of decreasing the criterion percent correct being used by that subject.

The runs thus had lengths that varied between 20 and 60 or more trials (with an average of ~30), according to when the criteria were met. The optimal values for termination criteria were ascertained by computer simulation of hundreds of runs and were also found to give psychophysical thresholds with close to the simulated variability even in untrained observers.

Evaluation of Staircase Performance

The performance of this pragmatic adaptive staircase was determined by both computer simulation studies and repeated runs by human observers. For the computer simulations, a Weibull slope of 3 was assumed for the psychometric function. A series of 250 runs was simulated with varying start points and the mean and the standard deviation of the final threshold estimates over all runs determined. The estimates for each run had a standard deviation of ±11% for run lengths averaging 30 trials, and the grand mean of the estimates was accurate within 2% of the assumed threshold (unbiased). In further simulations for starts as much as 1 log unit away from threshold, the average final thresholds were independent of the start point to within 0.02 log unit. The performance of human observers on 7 series of 10 runs at each temporal frequency showed similar standard deviations averaging 12%. These values may be compared with simulations of Watson and Pelli's[43] maximum-likelihood QUEST algorithm in a YES/NO format, which produced standard deviations of ±10% in runs averaging 30 trials,[44] under the assumption of the same psychometric function. For a two-alternative, forced-choice (2AFC) task, QUEST

had standard deviations approximately twice as high and required approximately twice as many trials to reduce the standard deviation to the YES/NO level.

The pragmatic adaptive staircase procedure was therefore approximately as efficient as the maximum likelihood approach but with much less computation. It was also robust against start points a considerable distance (as much as factor of 10) away from the threshold value. Compared with the maximum-likelihood 2AFC procedure, the pragmatic adaptive staircase is approximately twice as efficient, and the controlled-criterion features ensure that the observers operated at similar points on the receiver operating characteristic curve without the penalty of the inefficiency of the 2AFC procedure.

APPENDIX B: ISOLATION OF THE R-CONE RESPONSE

Eisner and MacLeod[50] performed heterochromatic flicker photometry (HCFP) with 15-Hz flicker of a 1.5°-diameter test spot set somewhere from 8% to 17% of the 2400-Td intensity of 7°-diameter background to which it was added. When an intense long-wavelength adapting background was used, the spectral sensitivity of the HCFP determination matched that of the G cones because their stimulus conditions were designed to desensitize the R-cone responses selectively as much as possible. The logic of their experiment was that the use of a moderate modulation amplitude and a low flicker frequency ensures that the dynamic retinal responses are in a range strongly affected by Weber-region adaptive behavior and that each receptor mechanism can be separately desensitized under appropriate adaptation conditions.

Ironically, however, this cone-isolation HCFP procedure has an inherent requirement that Weber's law adaptation should not be obeyed by the unadapted (or less adapted) cone mechanism being measured. If it were obeyed, then sensitivity to the flicker increment would be independent of the base intensity level, since the two remain in a constant proportion. Adjusting the relative intensities of the two lights of different wavelengths would have no effect on the perceived flicker, since the adaptation process would fully compensate for any change in intensity, resulting in a constant output as long as the modulation amplitude remained constant.

In summary, the Eisner–MacLeod cone isolation procedure makes the following assumptions:

(1) Each cone response is sufficiently adaptable that it can be made less sensitive than the other types over the full range of measurement.

(2) The unadapted (or less adapted) cone mechanism being measured is responding in a range where it is not affected by adaptation, since any degree of adaptation in proportion to its change in intensity would distort the estimate of its spectral sensitivity.

(3) The suprathreshold perception of flicker is directly proportional to the amplitude above threshold with the same slope for each cone mechanism throughout the measured spectrum.

(4) The spectral sensitivity is independent of temporal frequency of stimulation:

To provide some indication of the problems faced by this method, consider their claim that a long-wavelength adaptation light has the effect that the HCFP spectral sensitivity is determined by the G cones at all wavelengths. This might be interpreted to mean that under the conditions used in our study, a 660-nm modulation on a 660-nm steady background, threshold is determined by the G cones rather than the R cones. However, as long as Weber's law is obeyed (with equal Weber fractions for the two cone systems), it is impossible to desensitize the response of one cone system below that of another by adaptation with a background field of the same wavelength composition as the test field.

On the assumption of a constant threshold at low background levels, if the R-cone system is 2 log units more sensitive than the G-cone system, then increasing background adaptation will narrow the gap for the first 2 log units above threshold, when the two systems will become equally sensitive as long as Weber's law holds. We have established that Weber's law holds up to the highest intensities currently available, at least for the 660-nm light. It is only when one can induce supra-Weber saturation behavior that the response of the nonsaturated system can be isolated from that of the saturated one. Thus the relevance of the Eisner–MacLeod results to our study is only to show that, if high-frequency flicker responses were subject to adaptation, and if we had used no other isolation conditions, then the sensitivities might have been equally determined by the R and G cones.

However, previous experiments and those reported in the present study indicate that when the flicker rate is increased to rates close to CFF (e.g., 50 Hz under their conditions), flicker responses become linear and are not subject to adaptive desensitization. Thresholds would then be determined by the mechanism with the greatest absolute sensitivity at the test wavelength (if all mechanisms had the same temporal properties). In addition, our design involves the use of 100% modulation, so that the entire stimulus is the test stimulus, and there is no separate adapting stimulus. Under such nonadaptation conditions, it would be hard to dispute that spectral sensitivity in the long-wavelength region is determined by the R cones. Moreover, we used equiluminant surround conditions that should have profoundly depressed any residual G-cone responses (see Section 2). Finally, even in the Eisner–MacLeod study[45] the results suggested that sensitivity with the longest-wavelength adaptation field was determined by the R cones rather than the G cones. For all these reasons, the 660-nm CFF functions are considered to be mediated solely by the R-cone pathway.

APPENDIX C: INFLUENCE OF PROBABILITY SUMMATION IN FLICKER DETECTION

Use of an envelope of fixed duration introduces more cycles as frequency increases. One question this raises is whether thresholds improve at higher frequencies as a result of the increased opportunity for probability summation with increasing numbers of modulation cycles within the envelope. This in turn raises the question of the unit over which probability summation occurs. Although the number of cycles increases with increasing frequency, the energy within each cycle is proportionately reduced. Thus, if the probability summation occurs over units of stimulus energy, the best

way to hold it constant is to retain the same envelope duration at all frequencies.

To illustrate the logistical difficulty of holding the number of cycles constant, suppose that we wish to have 10 cycles within the high-amplitude (>50%) portion of the envelope. At 100 Hz, this would imply that the duration of the envelope at half-height should be 100 msec, for a total duration of 200 msec. To present a 1-Hz stimulus with the identical wave shape, an envelope duration of 10 sec would be required.

More formally, it can be shown that the effect of probability summation is equated for envelopes of fixed duration as frequency varies (just as is the Fourier energy). Probability summation in detection probability over n equal mechanisms of sensitivity s_i may be represented[46] by the Weibull function

$$P(c) = 1 - y \exp[-n(s_i c)^{\beta}], \tag{C1}$$

where c is contrast, y is the guessing level, and β is a parameter that determines the steepness of the psychometric function $P(c)$. For the integration of detection probability over time for a continuous stimulus waveform, the expression within the exponential brackets may be replaced by the integral

$$R = \int |Sf(t) * h(t)|^{\beta} dt, \tag{C2}$$

where S is the average sensitivity (assumed constant over time) and $f(t) * h(t)$ is the convolution of the stimulus waveform with the impulse response of the visual system up to the site of detection.[27,47] To the extent that $f(t)$ is a sine wave varying slowly with respect to the duration of the visual impulse response, the convolution term $C(t)$ will amount to a simple rescaling of the stimulus amplitude in proportion to the visual response sensitivity S_w at the temporal frequency of the stimulus:

$$C(t) = f(t) * h(t) = S_w \sin(wt). \tag{C3}$$

Thus, if the stimulus consists of many cycles of a sine wave within a raised-cosine envelope, the response will be of the same form:

$$C(t) = S_w[1 + \cos(t)]\sin(wt). \tag{C4}$$

The power integral [Eq. (C2)] of the response to the cosine-modulated sine wave of Eq. (C4) is intractable in the general case, but the problem may be solved by substitution of a Gaussian envelope for the raised cosine. This substitution has three advantages: an analytic solution is possible, it permits a sufficiently close approximation that the effects of probability summation should be similar for the two cases, and the solution is valuable for other applications in which the envelope was in fact a Gaussian (as is common for spatially modulated stimuli). The analysis will be further limited to an integral number of cycles, n, within the envelope.

Thus we assume that Gaussian modulation gives rise to an internal response at the site of detection of the form

$$R = \int_{-2\pi}^{2\pi} |\exp(-t^2/\pi) S_w \sin(nt)|^{\beta} dt, \tag{C5}$$

where n is the number of cycles within the envelope. Substituting an even integer for β and adjusting the integration limit to match tabulated solutions produces

$$R \sim 2S_w \int_0^{\infty} \exp(-2mt^2/\pi)\sin^{2m} nt dt. \tag{C6}$$

Expanding the power sine expression by the multiangle formula gives

$$\sin^{2m} nt = A_m\{1 + a_1 \cos(2nt) + a_2 \cos(4nt) \ldots + a_m \cos(2mnt)\}, \tag{C7}$$

from which it can be shown that

$$R = S_w \frac{A_m \pi}{\sqrt{2m}} \left\{1 + \sum_{k=1}^{m} a_k \exp[-\pi(2kn)^2/8m]\right\}. \tag{C8}$$

This expression consists of a constant followed by a finite series of exponentials controlled by the power of the integration (m) and the number of cycles under the envelope (n). Even for the lowest value of $k = 1$, these exponentials tend to 0 when the power is greater than 1 and the number of cycles exceeds the power, when

$$R \sim S_w \frac{A_m}{\sqrt{2m}}, \qquad n > m > 1. \tag{C9}$$

For example, under typical experimental conditions $B = 4$, $m = 2$, and the constants take the values $A_m = 3/8$, $a_1 = 4/3$, and $a_2 = 1/3$. For $n = 2$ the first term of the Gaussian expansion then takes the value 0.06, which is just greater than 5% of the constant term. Thus the Gaussian terms may be neglected for any number of cycles greater than 2 in this case, implying that the stimulus detectability is independent of the number of cycles under the assumptions of this analysis. This derivation therefore indicates that the effects of probability summation are proportionate to the duration of the envelope rather than to the number of cycles within it (above a small minimum value). The generality of the derivation suggests that this conclusion would apply equally to a nonlinear threshold detector ($\beta \gg 0$) as to a linear energy summator ($\beta = 1$).

A consequence of this conclusion is that holding the number of cycles constant, as did Stromeyer *et al.*,[31] decreases the stimulus energy in proportion to frequency. They used stimuli with a half-bandwidth of 6 cycles, which therefore corresponded to 600 msec at 10 Hz but only to 120 msec at their highest frequency of 50 Hz. It is therefore hardly surprising that they found saturation at higher frequencies earlier than the present data.

APPENDIX D: ON PHYSICAL REALIZABILITY: IRRELEVANCE OF THE PALEY-WIENER CRITERION

Kelly[15] has raised the question of the physical realizability of an equation describing visual response behavior, such as the Ferry–Porter law. The question arises in the interpretation of the equation as a frequency response amplitude function. To be physically realizable, the system that gave rise to the amplitude function must exhibit causal behavior; there must be no response preceding the time of the stimulus. This requirement sets a constraint on the range of allowable am-

plitude response functions. Mathematically, the constraint can be defined by the Paley–Wiener criterion that, for the frequency response amplitude function to derive from a causal system, the integral

$$\int_{-\infty}^{\infty} \frac{|\log[A(s)]|}{1+s^2}, \tag{D1}$$

where s is the complex frequency, must converge to a finite quantity. For this to occur, the log of the amplitude function must decline faster than frequency s in both positive and negative directions. This criterion implies the requirement that, when expressed in terms of negative exponentials, $\exp(-s^p)$, the power (p) of the complex frequency (s) is less than 1.

If a frequency response amplitude function does not meet this criterion of the convergence of the Paley–Wiener integral at infinity, then mathematically it can be shown that the corresponding impulse response will have some energy before t_0, i.e., a failure of causality. No set of phase relations between the frequency components will produce causal behavior. The Ferry–Porter law corresponds to an amplitude function with an exponential power of exactly 1 and must therefore be regarded as having no causal impulse response as an explicit mathematical solution, on the basis of its failure to meet the Paley–Wiener criterion.[15]

However, the Paley–Wiener criterion may be rejected as invalid for application to physical systems on three levels: theoretical, practical, and empirical. Theoretically, to be physically realizable the mathematical criterion must be applicable to a finite physical system. All physical systems have limits beyond which the integral expression becomes meaningless because it reaches the quantum limit of the atoms of which the system is constructed. In the case of light stimulation, it makes little sense to extend the integration limits beyond the frequency of the light waves with which the eye is stimulated (i.e., the gigahertz range). Thus an integral criterion that relies on infinite integration cannot in principle be applied to an inherently finite physical system. Conversely, if the integral is limited to a finite range, then the question of its convergence at infinity is indeterminate, and the Paley–Wiener criterion is inapplicable.

Second, even if the theoretical objection could be overcome by finding a physical system that permitted integration over an infinite range of frequencies, the Paley–Wiener criterion may be rejected on practical grounds for any function fitted to data over a specified frequency range. Regardless of the form of the function within this specified range, it will always be possible to find an extension of the function outside the specified range that would permit convergence of the integral.[48] Thus any theoretical function for the amplitude response over a finite frequency range is physically realizable, as long as an appropriate adjustment is permitted outside the specified range. One way to specify the range is to take it to the limit permitted by the noise inherent in any physical system. Beyond this limit the response is indeterminate because it is buried in noise, so that it may be said that any noise-limited frequency response could be physically realizable, since an appropriate adjustment could always be made in the range where the response is indeterminate.

Finally, any measured amplitude response function (or well-behaved theoretical function) may be fitted to any desired degree of accuracy over a specified range by a physically realizable approximation. This empirical approach is usually achieved by means of Bode analysis, in which the approximation is constructed from complex poles in the Fourier domain, each having a causal impulse response behavior. With a sufficient number of poles, any amplitude function may be approximated and therefore shown to be physically realizable within the degree of approximation. If the amplitude response function is measured over the full operational range of the system (e.g., up to the noise limit), then any expression completely describing the amplitude function within the accuracy of the noise may be said to be physically realizable.

Thus we conclude that the Paley–Wiener criterion is a mathematical abstraction that is not applicable to physical systems. The approximation of the Ferry–Porter law by an 8-pole filter model over a 5-log-unit operating range in Fig. 10 shows that the law is physically realizable in practice to a high degree of accuracy. Moreover, the use of a similar, 6-pole filter model for individual cone responses[39] shows that the Ferry–Porter law is compatible with an impulse response form that is close to that recorded physiologically from retinal receptors.

ACKNOWLEDGMENTS

Our thanks to Maureen Clarke for the programming and for the staircase simulations and to Richard Miller for contributions to the mathematical analysis. This research was supported in part by National Science Foundation grant BNS 8511099 and National Institutes of Health grants 1P30 EY 6883 and RR 5981.

REFERENCES

1. E. S. Ferry, "Persistence in vision," Am. J. Sci. **44**, 192–207 (1892).
2. J. Plateau, "Sur un principe de photometrie," Bull. Acad. R. Sci. Bell. Lett. Brux. **2**, 52–59 (1835).
3. T. C. Porter, "Contributions to the study of flicker," Proc. R. Soc. London Ser. A **70**, 313–329 (1902).
4. H. E. Ives, "Studies in the photometry of lights of different colours. II. Special luminosity curves by the method of critical frequency," Phil. Mag. **24**, 352–370 (1912); "Critical frequency relations in scotopic vision," J. Opt. Soc. Am. **6**, 254–268 (1922); "A theory of intermittent vision," J. Opt. Soc. Am. **6**, 343–361 (1922).
5. S. Hecht and S. Shlaer, "Intermittent stimulation by light V. The relation between intensity and critical frequency for different parts of the spectrum," J. Gen. Physiol. **19**, 965–979 (1936).
6. R. T. Brooke, "The variation of critical fusion frequency with brightness at various retinal locations," J. Opt. Soc. Am. **41**, 1010–1016 (1951).
7. D. H. Kelly, "Visual responses to time-dependent stimuli. I. Amplitude sensitivity measurements," J. Opt. Soc. Am. **51**, 422–429 (1961); "Sine waves and flicker fusion," in *Flicker*, H. E. Henker and L. H. van der Tweel, eds. (Junk, The Hague, 1964), pp. 16–35.
8. S. Hecht and C. D. Verrijp, "Intermittent stimulation by light. III. The relation between intensity and critical fusion frequency for different retinal locations," J. Gen. Physiol. **17**, 251–268 (1933).
9. R. T. Brooke, "The variation of critical fusion frequency with brightness at various retinal locations," J. Opt. Soc. Am. **41**, 1010–1016 (1951).
10. R. B. Pinter, "Sinusoidal and delta function responses of visual cells of the limulus eye," J. Gen. Physiol. **49**, 565–593 (1966).

11. D. Tranchina, J. Gordon, and R. M. Shapley, "Retinal light adaptation—evidence for a feedback mechanism," Nature (London) **310,** 314–316 (1984).
12. S. J. Daly and R. A. Normann, "Temporal information processing in cones: effects of light adaptation on temporal summation and modulation," Vision Res. **25,** 1197–1206 (1985).
13. G. A. Oesterberg, "Topography of the layer of rods and cones in the human retina," Acta Ophthalmol. Suppl. **VI** (1935).
14. S. Polyak, *The Retina* (U. Chicago Press, Chicago, Ill., 1941).
15. D. H. Kelly, "Diffusion model of linear flicker responses," J. Opt. Soc. Am. **59,** 1665–1670 (1969).
16. F. Veringa, "Enige natuurkundige aspecten van het zien van gemoduleerd licht," Ph.D. dissertation (University of Amsterdam, Amsterdam, 1961).
17. A. Charpentier, *Recherches sur la Persistence des Impressions Retiniennes et sur les Excitations Lumineuses de Courte Durée* (Steinheil, Paris, 1890).
18. P. Lasareff, "Theorie der Lichtreizung der Netzhaut beim Dunkelsehen," Pflugers Archiv. Gesamte Physiol. Menschen Tiere **154,** 459–469 (1913).
19. J. Z. Levinson and L. Harmon, "Studies with artificial neurons. III. Mechanism of flicker fusion," Kybernetik **1,** 107–117 (1961).
20. D. H. Kelly, R. M. Boynton, and W. S. Baron, "Primate flicker sensitivity: psychophysics and electrophysiology," Science **194,** 1077–1081 (1976).
21. C. W. Tyler, "Analysis of visual modulation sensitivity. III. Meridional variations in peripheral flicker sensitivity," J. Opt. Soc. Am. A **2,** 1612–1619 (1987).
22. W. S. Stiles, "The directional sensitivity of the retina and the spectral sensitivities of the rods and cones," Proc. R. Soc. London Ser. B **127,** 64–105 (1939).
23. J. L. Schnapf, T. W. Kraft, and D. A. Baylor, "Spectral sensitivity of human cone photoreceptors," Nature (London) **325,** 439–441 (1987).
24. L. O. Harvey, "Flicker sensitivity and apparent brightness as a function of surround luminance," J. Opt. Soc. Am. **60,** 860–864 (1970).
25. S. P. McKee and G. Westheimer, "Specificity of cone mechanisms in lateral interaction," J. Physiol. **203,** 117–128 (1970).
26. G. J. C. van der Horst and M. A. Bouman, "Spatiotemporal chromaticity discrimination," J. Opt. Soc. Am. **59,** 1482–1488 (1969).
27. A. Gorea and C. W. Tyler, "New look at Bloch's law for contrast," J. Opt. Soc. Am. A **3,** 52–61 (1986).
28. A. Ransom-Hogg and L. Spillman, "Perceptive field size in fovea and periphery of the light- and dark-adapted retina," Vision Res. **20,** 221–228 (1980).
29. R. Granit and P. Harper, "Comparative studies on the peripheral and central retina. II. Synaptic reactions in the eye," Am. J. Physiol. **95,** 211–227 (1930).
30. C. W. Tyler, "Analysis of visual modulation sensitivity. II. Peripheral retina and the role of photoreceptor dimensions," J. Opt. Soc. Am. A **2,** 393–398 (1985).
31. C. F. Stromeyer III, G. R. Cole, and R. E. Kronauer, "Chromatic suppression of cone inputs to the luminance flicker mechanism," Vision Res. **27,** 1113–1137 (1987).
32. S. Hecht and C. D. Verrijp, "Intermittent stimulation by light. IV. A theoretical interpretation of the quantitative data of flicker," J. Gen. Physiol. **17,** 269–282 (1933).
33. J. M. van Buren, *The Retinal Ganglion Cell Layer* (Thomas, Springfield, Ill., 1963).
34. D. H. Kelly, "Retinal inhomogeneity. I. Spatiotemporal contrast sensitivity," J. Opt. Soc. Am. A **1,** 107–113 (1984).
35. J. Rovamo and V. Virsu, "An estimation and application of the human cortical magnification factor," Exp. Brain Res. **37,** 495–510 (1979).
36. B. M. Dow, A. Z. Snyder, R. G. Vautin, and R. Bauer, "Magnification factor and receptive field size in foveal striate cortex of the monkey," Exp. Brain Res. **44,** 213–228 (1981).
37. J. G. Robson, "Spatial and temporal contrast-sensitivity functions of the visual system," Nature (London) **564,** 1141–1142 (1966).
38. H. de Lange, "Experiments on flicker and some calculations on an electrical analogue of the foveal systems," Physica **18,** 935–950 (1952); "Research into the dynamic nature of the human fovea–cortex systems with intermittent and modulated light. I. Attenuation characteristics with white and colored light," J. Opt. Soc. Am. **48,** 777–785 (1958).
39. D. A. Baylor, A. L. Hodgkin, and T. D. Lamb, "Reconstruction of the electrical responses of turtle cones to flashes and steps of light," J. Physiol. **242,** 685–727 (1974).
40. A. Raninen and J. Rovamo, "Perimetry of flicker frequency in human rod and cone vision," Vision Res. **26,** 1249–1256 (1986).
41. E. Wolf and R. J. Vincent, "Effect of target size on critical flicker frequency in flicker perimetry," Vision Res. **3,** 523–529 (1963).
42. B. Dreher, Y. Fukuda, and R. W. Rodieck, "Identification, classification and anatomical segregation of cells with X-like and Y-like properties in the lateral geniculate nucleus of old-world primates," J. Physiol. **258,** 433–452 (1976).
43. A. B. Watson and D. Pelli, "A Bayesian adaptive psychometric method," Percept. Psychophys. **33,** 113–120 (1983).
44. R. Madigan and D. Williams, "Maximum likelihood psychometric procedures in two-alternative forced-choice: evaluation and recommendation," Percept. Psychophys. **42,** 240–249 (1987).
45. A. Eisner and D. I. A. MacLeod, "Flicker photometric study of chromatic adaptation: selective suppression of cone inputs by colored backgrounds," J. Opt. Soc. Am. **71,** 705–718 (1981).
46. A. B. Watson, "Probability summation over time," Vision Res. **18,** 515–522 (1979).
47. R. F. Quick, "Vector magnitude model of contrast detection," Kybernetik **16,** 65–67 (1974).
48. D. G. Stork and D. S. Falk, "Temporal impulse responses from flicker sensitivities," J. Opt. Soc. Am. A **4,** 1130–1135 (1987).